PACS: 61.20.-p

F.E. Leys[1], N.H. March[1,2], F. Perrot[3], G. Straub[4], and V.E. Van Doren[1]

VARIATION OF LOCAL COORDINATION NUMBER WITH THERMODYNAMIC STATE IN ELEMENTAL LIQUIDS INCLUDING METALS

[1] Physics Department, University of Antwerp (RUCA)
Groenenborgerlaan 171, B-2020 Antwerpen, Belgium

[2]Oxford University, Oxford, UK

[3]Commissariat à l'énergie atomique, Centre de Bruyères le Châtel
Boîte Postale 12, 91680 Bruyères le Châtel, France

[4]Theoretical division, Los Alamos National Laboratory
Los Alamos, NM 87545, USA

Local coordination numbers can be estimated from liquid structure factors by a number of routes. Here, we keep as close as possible to the liquid structure factor S(q) data, determined by diffraction experiments. For the expanded fluid heavy alkali metals along the liquid-vapour coexistence curve towards the critical point, the coordination number varies linearly with number density. Here attention is focused also on the melting curve of Rb under pressure, the results being compared and contrasted with the predictions of the one-component plasma model (OCP). Such liquid alkali metal behaviour is then compared and contrasted with that of some highly directionally bonded fluids including B,C and Si, in the latter two of which liquid-liquid phase transitions occur in very different regimes of thermodynamic state.

Finally, some structural integrals involving pair potentials and the pair correlation functions they generate are used to define a characteristic 'structural length'. In turn, this is compared with a 'thermodynamic length' which is defined as the ratio of surface tension to the deviation of the pressure P from its perfect gas value $\rho k_B T$ *. Some numerical results are given utilizing pair potentials and corresponding structure factors for Be and B.*

I. BACKGROUND AND OUTLINE

Winter et al. [1,2], in pioneering neutron diffraction studies on the structure factors $S(q)$ of liquid metallic Rb and Cs, considered a number of thermodynamic states along the liquid-vapour coexistence curve towards the critical point. One major finding of their studies was that the high coordination numbers just above the freezing point, compatible with the local coordination in hot bcc crystals, were progressively reduced as these two heavy alkali metallic liquids were highly expanded. From the same experimental structure data, it was found for liquid Cs that the near-neighbour distance was relatively constant, as the density is lowered, which lends support to the view that a chemical bond is the basic building block in these expanded fluid states [3]. For liquid Rb, however, the near-neighbour distance remains constant only up to T = = 1200 K. Both the experimental results [4] and results from molecular dynamics simulations [5] can be fitted by the linear relation

$$z = \alpha\rho + \beta \tag{1}$$

where z denotes the number of near neighbours or the main coordination number and ρ is the number density. Depending on the formula used to derive z from the pair correlation function $g(r)$, this relation predicts values for z at the critical point ranging from two [4] to about 4.5 [5].

Subsequent to the experiments of Winter et al. further studies of Rb have been reported, but now along the melting curve under pressure. These will be the focus of section two below, where some insight is gained into the changes in liquid structure factors with pressure in Rb by invoking the one-component plasma (OCP) model [6,7]. Section three will then be concerned with comparing and contrasting the properties of nearly free liquid metals with those of some highly directionally bonded fluids, including liquid B and C. In particular, liquid-liquid phase transitions (LLPT) in both liquid C and Si will be one focal point. Some brief discussion of the melting curve of Ar will also be reported, where a comparison will be made with a model of such melting curves derived from inverse n-power repulsive pair potentials. Two lengths, one thermodynamic and one structural will be defined and discussed in Section 4 while Section 5 constitutes some suggestions for possible future studies.

II. STRUCTURE AND COORDINATION OF Rb ALONG ITS MELTING CURVE UNDER PRESSURE

A. Comparison with bare OCP model

In a recent paper by Shimojo et al. [8] the effects of pressure on the structural and electronic properties of liquid Rb were studied along its melting curve using ab-initio molecular dynamics (MD). Simulations were carried out for three different thermodynamic states along the melting curve for which the values of density and temperature are given by (0.010 $Å^{-1}$, 350 K) near the triple point, (0.015$Å^{-1}$, 520 K) and (0.020$Å^{-1}$, 570 K) corresponding to pressures of 0, 2.5 and 6.1 GPa, respectively. Over this pressure range good agreement with experiment was found.

Since the structure factors $S(q)$ and pair correlation functions $g(r)$ of liquid alkali metals have highly symmetric peaks, the method of 'symmetric main maximum' [2] was used to define the local coordination number z:

$$z = 2\rho \int_0^{R_m} g(r) 4\pi r^2 \, \mathrm{d}r \tag{2}$$

with R_m the position of the first maximum of $g(r)$. It must be noted explicitly, however, that there is a degree of arbitrariness in the definition of z. An alternative formula which is frequently used [9] is

$$z = \rho \int_0^{R_{\min}} g(r) 4\pi r^2 \, \mathrm{d}r \tag{3}$$

where R_m now denotes the position of the first mininum after the first peak of $g(r)$. Inspired by eqn. (1) we rewrote eqn. (2) as follows

$$z = 2\left(\frac{4}{3}\pi R_m^3\right)\rho + \frac{4R_m^2}{\pi}\int_0^\infty (S(q)-1)j_1(qR_m)q\,\mathrm{d}q \qquad (4)$$

with $j_1(qR_m)$ the first-order spherical Bessel function. This formula has the obvious merit that starting from e.g. an experimental $S(q)$, only one integral needs to be evaluated, plus, however, determination of R_m. From the experiments of Winter et al. R_m = 5.2 Å along the liquid-vapour coexistence curve of Cs and inserting this value into the first term of the right-hand side of eqn. (4) gives a coefficient of about 636 Å^3. However using eqn. (1) to fit experiment gives a value for α of about 1177 Å^3. This reveals still a considerate density dependence of the integral on the right-hand side of eqn. (4) along the liquid–vapour coexistence curve.

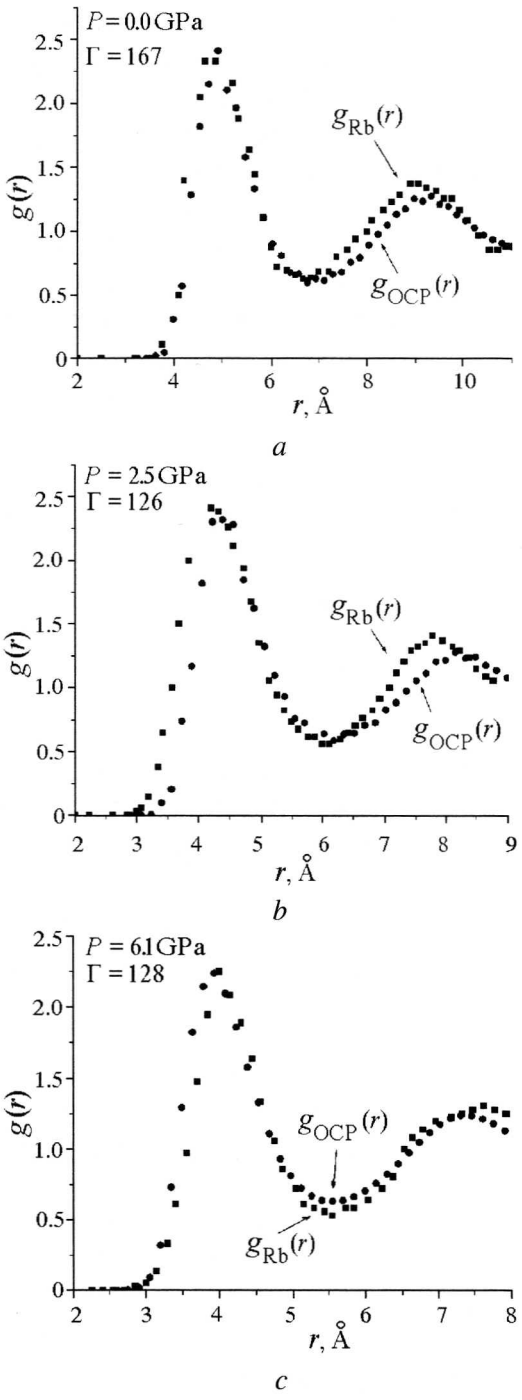

Fig. 2.1. $g_{OCP}(r)$ and $g_{MD}(r)$ for liquid Rb along the melting curve under pressure

Shimojo et al. found that liquid Rb is compressed uniformly up to 2.5 GPa, the local coordination number z remaining constant at its solid bcc (the structure from which Rb melts under atmospheric pressure) value of 8. In going from 2.5 to 6.1 GPa the local coordination number increases to about 11, indicating a structural change to a denser structure. They then decomposed the electronic density of states into its angular momentum eigenstates $D_l(E)$ and found that, as the pressure increases, the *d*-component near the Fermi level becomes gradually more important (at the cost of a decrease of the *s*-component), going from a very small contribution near the triple point to the main contribution at 6.1 GPa.

The effective ion-ion potential in monovalent metals such as Na is known to be rather soft compared to polyvalent metals such as Al. For this reason the OCP-reference system has proven to give a lower variational bound to the free energy and a better fit to the experimental structure factor of liquid Na

and Li [10] than does the hard-sphere fluid. Liquid Al, however is found to be described better by the hard-spheres reference system. The focal point here therefore is to examine how well the OCP pair correlation function $g_{OCP}(r)$ generates the main features of the MD pair correlation $g_{MD}(r)$ for liquid Rb at atmospheric pressure and how this evolves as one goes to higher pressures. More specifically we have examined the OCP predictions for the local coordination number z and the position of the first peak of the pair correlation function.

The values for the coupling strength Γ for the three thermodynamic states with increasing pressure are approximately $\Gamma = 167, 126$ and 128. The $g_{OCP}(r)$'s at these values for Γ were obtained by interpolating between the $g_{OCP}(r)$'s that Hansen [7] calculated from MD-simulations of the one-component plasma for a different set of Γ-values. Figs. 2.1, *a*, *b* and c show the $g_{MD}(r)$'s for the three states respectively compared with the relevant $g_{OCP}(r)$'s. Good overall agreement is found although that the first peak is better reproduced than the second one.

We notice from Fig. 2.2,*a*, which shows the position of the first peak in $g(r)$ as a function of $\left(\frac{V}{V_0}\right)^{\frac{1}{3}}$, V_0 being the equilibrium volume at atmospheric pressure, that up to 2.5 GPa the OCP curve and the Rb curve run closely parallel, confirming that Rb is compressed uniformly. For pressures between 2.5 and 6.1 GPa there is a clear deviation from uniform compression, the two curves now crossing each other. Using definition (2) to calculate the coordination number z we find that z remains roughly at a constant value of about 7, close to 8, the value for the bcc-structure from which the classical OCP melts at $\Gamma = (155 \pm 10)$ [7]. Fig.(2.2, *b*) shows and contrasts the predictions for the coordination number from the MD-simulations of liquid Rb and those for the OCP.

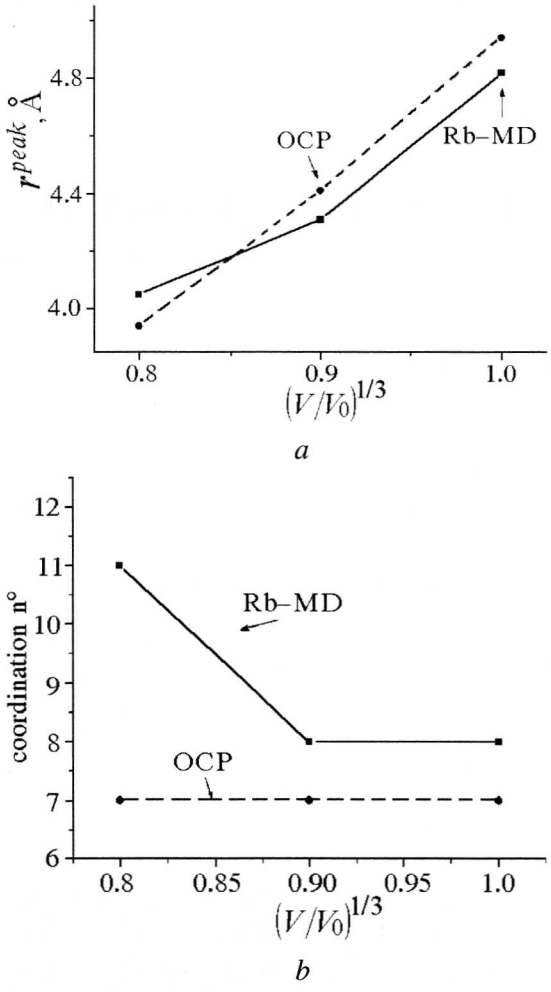

Fig. 2.2. Comparison between OCP predictions and results from MD simulation of liquid Rb. (*a*) for the position of the first peak of $g(r)$ and (*b*) for the coordination number z

Thus we conclude that the change of state of the electrons does not influence significantly the values of the near neighbour distance between the ions although it does cause a slight change in slope indicating a departure from uniform compression. Also the height of the first peak, although this height, contrary to that of the first

peak of $S(q)$, does not have a very direct physical interpretation, is reproduced quite accurately. That the change in coordination number is not reproduced correctly by the OCP should occasion no surprise since we know that in the real liquid the change in z is driven by an electronic *s-d* transition while the electrons in the OCP are simulated by a uniform background.

B. Electronic effects incorporated into OCP model

We now discuss briefly how we can incorporate those electronic effects to go analytically from the OCP-structure factor S_{OCP} to the real structure factor $S(q)$. Since the pair correlation function $g(r)$ is essentially the Fourier transform of $(S(q)\text{-}1)$ this should give information of screening effects on local coordination. The simplest possible inclusion of screening effects is the random phase approximation (RPA) which assumes that the interference of all correlations with third particles in the liquid is destructive, not only at large distances but also at small and intermediate distances. In this approximation the following general formula is obtained between the structure factor and the assumed pair potential ϕ [31]:

$$S(q)=\left(1+\frac{\rho\phi(q)}{k_BT}\right)^{-1}. \tag{5}$$

In *sp*-bonded liquid metals the effective pair potential in q-space $\phi(q)$ can be written as the sum of the direct Coulomb repulsion between the ions plus an indirect term coming from the screening correction i.e.

$$\phi(q)=\frac{4\pi e^2}{q^2}+\bar{v}(q) \tag{6}$$

with

$$\bar{v}(q)=\frac{V_{ei}^2(q)}{4\pi e^2/q^2}\left(\frac{1}{\varepsilon(q)}-1\right) \tag{7}$$

$\varepsilon(q)$ being the Lindhard dielectric function and $V_{ei}(q)$ the Fourier transform of the electron-ion pseudopotential. Inserting the decomposed expression (6) into eqn. (5) and applying the RPA in the OCP as well as in the metal leads to the following formula

$$S(q)=\frac{S_{OSP}^{RPA}(q)}{1+\frac{\rho\bar{v}(q)}{k_BT}S_{OSP}^{RPA}(q)} \tag{8}$$

One can now insert into this equation a structure factor obtained from computer experiment on the OCP in order to (hopefully) get a better approximation for $S(q)$ then if one would use only eqn. (5). Obviously, because of the underlying physical assumptions eqn. (8) is only valid in the small-angle scattering region and unfortunately already gives meaningless results for the first peak of $S(q)$. As Senatore and Tosi [11] pointed out, this can be remedied by introducing an empirical cut off of the screening

correction $\bar{v}(q)$ at the first node of $V_{ei}(q)$, a procedure which can be reconciled with the optimized random phase approximation (ORPA). However these formulae start from the assumption of a spherical Fermi-surface and weak scattering, assumptions which are unjustified when the valence electrons start to occupy (partly) directional and resonant d-states as is the case in liquid Rb under pressure.

We conclude by noting that the behaviour of liquid Rb under pressure is in sharp contrast with that of liquid Na for which, as the experiments of V.A. Ivanov et al. [12] pointed out, the coupling strength Γ along the melting curve under pressure tends to the value of 155, the value of Γ for which the classical OCP melts [7]. This shows that, up to the measured pressures, Na remains a nearly free electron metal, in fact becoming more uniform as one goes to higher pressures. So in contrast to Rb, screening effects which change the interatomic potential become less important as we go to higher pressures.

C. Inverse power pair potentials: melting of Ar and K

A more general class of reference systems, of which the bare Coulomb force and the hard spheres are special cases, are the inverse power pair potentials proportional to $\frac{1}{r^n}$. It is of interest in the light of the above discussion of the melting curve of Rb under pressure to briefly record results on the corresponding curve of Ar. The experimental melting curve is shown in Fig. (2.3). For comparison we have plotted the Simon melting curve [13]

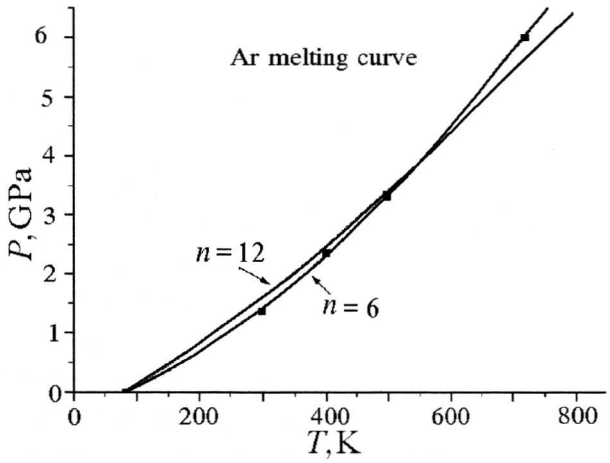

Fig. 2.3. Melting curve of Ar: experimental values [14] (dots) compared with Simon melting curve for $n = 6$ and $n = 12$ respectively (solid lines)

$$P - P_0 = a\left(\left(\frac{T}{T_0}\right)^{1+\frac{3}{n}} - 1\right) \qquad (9)$$

which has been proved to be exact for inverse power repulsive potentials. The experimental curve is reproduced exactly choosing $a = 0.23$ and $n = 6$. The best possible fit, obtained by forcing n to be equal to 12 is also shown in the plot. Though the repulsive part of the potential in Ar is roughly like $\frac{1}{r^{12}}$ presumably the better fit with $n = 6$ is mimicking a compromise between pure repulsion and Van der Waals attraction. Using eqn. (9) to fit the melting curve of Rb leads to an unphysical value for n of 0.34. For Ar we conclude that although the hard sphere phase diagram already has a melting curve, the attractive term does influence the shape of the melting curve.

III. COORDINATION NUMBER CHANGES IN CHEMICALLY BONDED LIQUIDS: B, C AND Si

The experiments of Tsuji [15] pointed out that the high pressure behaviour of covalently bonded liquid metals or semiconductors differs substantially from that of the nearly free electron metals considered in the previous section. Application of pressure to covalently bonded liquid metals causes existing bonds to break and new bonds to form and, as a consequence, the position of the first peak of $g(r)$ can remain constant or even shift towards larger values, in spite of the compression. These facts inspired us first to look at theoretical predictions of similar changes in covalent bonds and the possible change in coordination numbers associated with them.

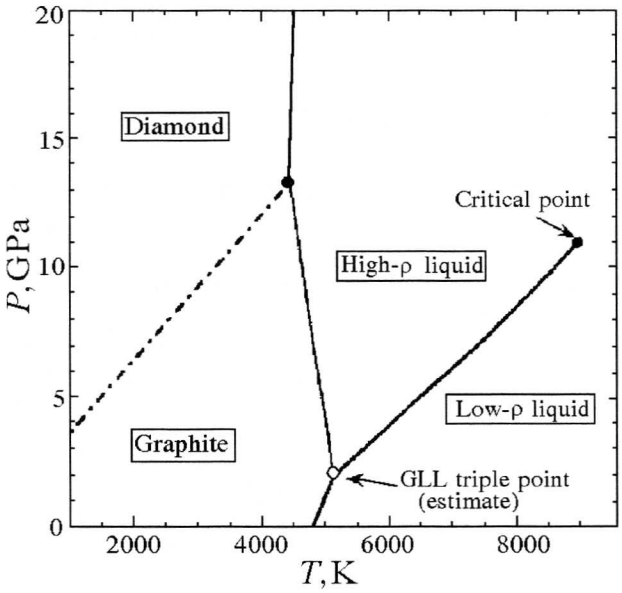

Fig. 3.1. Carbon phase diagram: The solid lines present the simulation results using atomistic simulations. The diamond-graphite line (dot-dash) was previously obtained by F.P. Bundy [18] (redrawn from ref. 17)

Ferraz and March [16] suggested in connection with the phase diagram of C the possibility of a liquid-liquid phase transition (LLPT) into a low-density liquid with *sp*-hybridization. Pioneering work of Glosli and Ree [17] using atomistic simulations with a bond-order potential has proved the existence of a first-order LLPT in C. Fig. (3.1) shows the carbon phase diagram now including the new phase line which starts at a triple point on the graphite melting line and is terminated by a critical point. They found that the phase change is associated with a change in density and in local structure; while the high-density liquid is mostly sp^3 bonded with little *sp* character, the low-density liquid is predominantly *sp* bonded with little sp^3 character [18].

Following this discussion of different hybridization states in different thermodynamic states of liquid C, we note also recent work, both experimental diffraction using containerless techniques involving electromagnetic levitation plus computer simulation studies. Continuous interest in the development of containerless techniques involving levitation has recently made it possible to gain access for the first time to materials with extremely high melting temperatures and high reactivity such as B in the liquid and supercooled state [19]. Pure boron melts at (2360 ± 10) K from the isolating β-

rhombohedral phase to a metallic liquid of which the precise structure is unknown. The structural unit in the solid phase is a 12-atom regular icosahedron which is positioned at the center and the vertices of a pentagonal pyramid giving rise to an *average* coordination number of 6.6. Both experiment [19] and MD simulations [20] agree on the fact that, in the liquid, boron has a relatively open structure with a coordination of about six, a number which remains fairly constant when the temperature is changed, except when going into the supercooled region when it rises to a value of 6.2.

The main question remains, however, whether the icosahedral units survive the melting transition. This was not the case in the MD-simulations from Vast et al. [20] but these calculations only simulated 48 atoms. According to Krishnan and Price, one of the indications that the icosahedrons survive is the surface tension of B, which is found to be low.

Table 3.1.

Changes in coordination z with thermodynamic state of liquid boron

Phase	T,K	z
Liquid	2600	5.8±1
Liquid	2400	5.8±1
Supercooled Liquid	2090	6.2±1
Liquid (MD-result)	2600	6.0

Liquid Si is metallic [21,22] and has a coordination number near to six, thus having also a relatively open structure compared to other liquid metals near their freezing points. The indication from this is that some directional bonding characteristics persist above the freezing temperature. This view is supported by studies of supercooled liquid Si [23]. The point to be stressed about Si in the present context, however, is that there is a significant but continuous lowering in local coordination number z with supercooling. Such a change in z found from diffraction measurements is consistent with MD-simulations [24]. These simulations, however, also reveal a LLPT in Si near the bulk supercooling limit from a metallic phase with coordination number 4.6 to a semiconductor phase with four-fold sp^3 coordination.

Then going into the inversion of the structure factor obtained from ab-initio MD by Vast et al. [20] at one thermodynamic state, following Reatto et al. [25], has led to the effective ion-ion pair potential shown in Fig. (3.2). For comparison, the electron

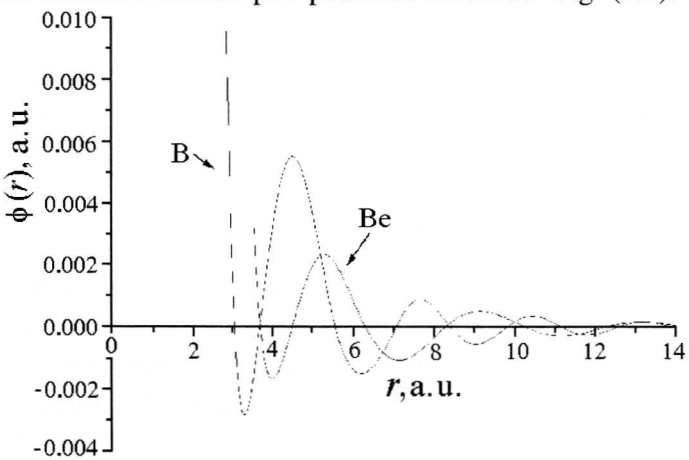

Fig. 3.2. Pair potentials for specific thermodynamic states of liquid B and Be. The former was obtained by Vast et al. [20] by inversion of a structure factor. The striking similarity between the attractive first minima and the subsequent and larger repulsive hump is the point to focus on here

theory plot of the high conductivity divalent liquid metal Be calculated by Perrot and March [26] is shown. An asymptotic tail of the form $\frac{\cos(2k_f r+\delta)}{r^3}$ was fitted to both potentials to extend their range. Remarkable qualitative similarities are in evidence, both materials having a repulsive hump which is higher than the depth of the first minimum. The possibility that Be has, just as B, a degree of directional bonding was clear from the early diffraction work of Brown [27] and from the theoretical work of Matthai et al. [28].

Inspired by the remark on the low surface tension σ of B, we attempted to use the pair potential and pair correlation function of Vast et al. to calculate σ by using the simplest possible formula, namely Fowlers formula (see eqn. (10) below). Using this formula we obtained however a negative value which is obviously incorrect, but a pointer towards a small value of σ. Before accepting this result three points need making. First of all, as Freeman et al. [29] noted, a straightforward calculation of structural integrals requires a very precise knowledge of the pair correlation function $g(r)$ and is therefore not the most appropriate way to proceed. Secondly, although a central pair potential is of course the best one can get from inverting a one dimensional structure factor, it is questionable how useful this is in a directionally bonded fluid such as B. And lastly, in the derivation of Fowler's expression for the surface tension, no explicit account was taken of contributions to the pressure in liquid metals coming from the volume dependence of the pair potentials and the volume-dependent, structure independent term. This leads us in the penultimate section to look further into some physical properties related to structural integrals.

IV. TWO LENGTHS

In early work, Fowler [30] derived the following (approximate) formula giving the surface tension σ in terms of a pair potential $\phi(r)$ and the liquid pair correlation function $g(r)$:

$$\sigma=\frac{\rho^2}{32}\int r^2\frac{\partial\phi}{\partial r}g(r)\,\mathrm{d}^3 r. \tag{10}$$

For comparison, we next write the virial equation of state

$$P=\rho k_B T-\frac{\rho^2}{6}\int r\frac{\partial\phi}{\partial r}g(r)\,\mathrm{d}^3 r. \tag{11}$$

Such structural integrals, generalized to

$$S_n=\int r^n\frac{\partial\phi}{\partial r}g(r)\,\mathrm{d}^3 r \tag{12}$$

are of continuing interest in elemental fluids such as Ar and K, where pair potentials are known to afford useful starting points even in dense fluids near their triple points. Plainly the ratio $\frac{S_2}{S_1}$ has dimensions of length, which may be termed a 'structural length' $\langle r\rangle_{st}$. In essence this formula can be interpreted as an expectation value of r. But eqns. (10) and (11) lead us to focus on the thermodynamic length which we shall define by

$$\langle r\rangle_{th} = \frac{\sigma}{\left(\rho k_B T - P\right)} \tag{13}$$

that is the ratio of the surface tension σ to the 'deviation ' (large for dense liquids) of the liquid pressure from its ideal gas limit. It is the definition (13) that is the focus of the present study. It is now instructive to introduce into eqn. (4) the relation

$$\sigma K_T = L \tag{14}$$

which has proved widely useful in dense liquids, K_T being the bulk isothermal compressibility and L having dimensions of length [31]. Introducing also the so-called compressibility ratio $Z = \frac{P}{\rho k_B T}$ into eqn. (13) one readily obtains the result that

$$\langle r\rangle_{th} = \frac{L}{\rho k_B T K_T (1 - Z)}. \tag{15}$$

But from fluctuation theory [31] one can re-express $\rho k_B T K_T$ as the long wavelength limit (q–>0) of the bulk liquid structure factor $S(q)$ (essentially the Fourier transform of $g(r) - 1$) to find

$$\langle r\rangle_{th} = \frac{L}{S(0)(1 - Z)}. \tag{16}$$

For a variety of liquid metals, $S(0)$ is known from experiment at the melting temperature T_m and this quantity $S_{T_m}(0)$ is recorded in Table (4.1) for some 20 such liquids. It is seen to range from 0.005 for Ga to 0.047 for Be, but for the 5 alkali metals Li–Cs it is almost contant ($\approx$0.025). Also the length L in the numerator is rather constant through the metals, ranging from about 0.15 to 0.5 Å. Taking therefore an average value for L of 0.3 Å in eqn. (16), then since $Z_{T_m} << 1$ for these alkali metals, $\langle r\rangle_{th}|_{T_m} \approx 10$ Å indicating that the length concerns intermediate range order. Taking eqn. (14) to define L, we have also entered some values of L from ref. [32] in Table (4.1), along with some values of $\left(\frac{L}{S(0)}\right)_{T_m}$. Both liquid Be and liquid Hg, the elements with respectively the smallest and the largest value for $\langle r\rangle_{th}$ have a relatively long ranged order in the liquid because of a large repulsive hump after the first minimum in the effective pair potential. We assume that it is due to interference effects in the integral expression for the structural length, which is approximately equal to the thermodynamic length at triple point conditions, both elements end up at different sides of the value spectrum for $\langle r\rangle_{th}$.

V. FUTURE DIRECTIONS

As to future directions, the dynamic structure factor $S(q,\omega)$ is an obvious candidate for future work. And indeed, for Rb, the liquid metal considered in most detail in the present study, the dynamic structure of this metal, under expansion (compare section 1) has been investigated by means of a molecular dynamics simulation [33]. The pair potential obtained by inverting the measured structure factor clearly emerges as

Table 4.1

Values for $\langle r \rangle_{th}$ calculated from experimental results for $S(0)$ at melting temperature and results for L taken from ref. [32]

Liquid metal	L, Å	$S(0)$	$\langle r \rangle_{th} \approx \frac{L}{S(0)}$, Å
Li	0.45	0.031	14.5
Na	0.37	0.023	16.0
K	0.42	0.023	18.2
Rb	0.42	0.022	19.1
Cs	0.48	0.024	20.0
Be	0.26	0.047	5.5
Mg	0.29	0.025	11.6
Ca	0.38	0.035	10.9
Sr	0.39	0.031	12.6
Ba	0.45	0.036	12.5
Cu	0.19	0.021	9.0
Ag	0.19	0.019	10.0
Zn	0.19	0.015	12.7
Cd	0.19	0.011	17.3
Hg	0.18	0.005	36.0
Al	0.21	0.017	12.4
Ga	0.16	0.005	32.0
In	0.17	0.007	24.3
Ti	0.18	0.010	18.0
Sn	0.15	0.007	21.4
Pb	0.16	0.009	17.8
Sb	0.19	0.019	10.0
Bi	0.16	0.009	17.8

favoured over its pseudopotential alternative, the former potential being able to reproduce quite well the dynamic structure factor of Rb over a wide range of densities up to near the critical density.

APPENDIX A

Local coordination number as an approximate constraint on the Ornstein-Zernike direct correlation function

Reatto et al. [25] have tabulated the direct correlation function $c(r)$, the pair correlation function $g(r)$ and the liquid structure factor $S(q)$ for a Lennard-Jones fluid with a pair potential $\phi_{LJ}(r)$ given by

$$\phi_{LJ}(r) = -4\varepsilon\left[\left(\frac{\sigma}{r}\right)^6 - \left(\frac{\sigma}{r}\right)^{12}\right] \tag{A.1}$$

under conditions at the triple point given by

$$\rho\sigma^3 = 0.84; \quad \frac{k_B T}{\varepsilon} = \frac{3}{4}. \tag{A.2}$$

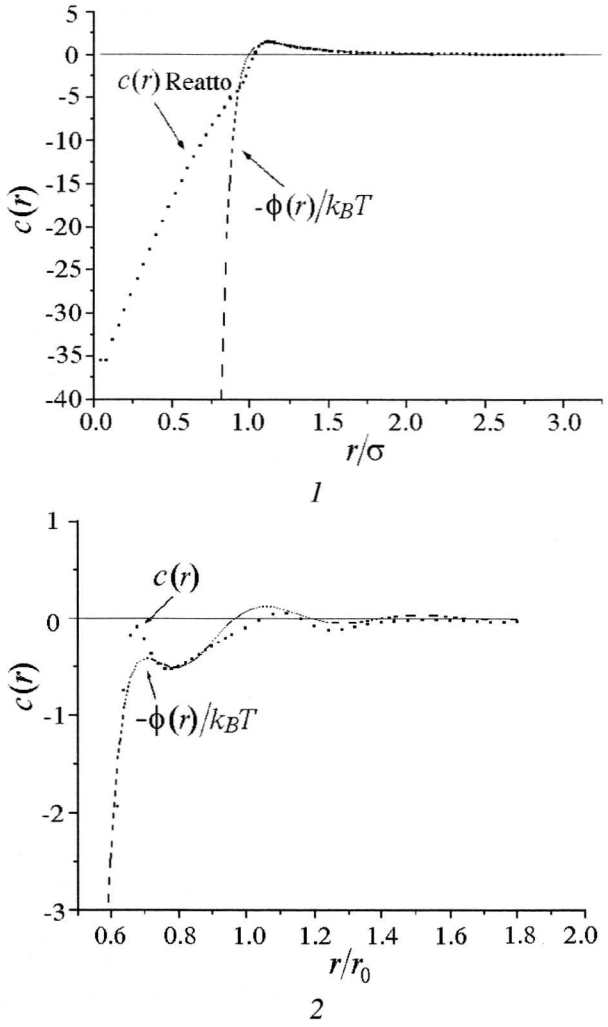

Fig. A. Plot of Ornstein-Zernike direct correlation function $c(r)$ (dots) from computer simulation by Reatto et al. [25]. 1) of a Lennard-Jones fluid 2) of liquid Al. The solid lines give in both cases the asymptotic result at large r

The structure was determined by molecular dynamics, with the potential cut off at 4σ. $g(r)$ however was extended by Verlet's algorithm [34] in order to obtain $c(r)$, which is plotted in Fig. (A.1). For comparison we also plotted the results obtained from a model potential for Al in Fig. (A.2).

Bhatia and March proposed the approximate result

$$zc(a)\big|_{T_m} \cong \left(\tilde{c}(q=0) - c(r=0) - 1\right) \tag{A.3}$$

where 'z' and 'a' refer to local coordintion number and near-neighbour distance in the hot solid near T_m. The argument given was appropriate to an insulator such as Ar. However, the removal of the conventional pair potential in favour of the direct correlation function makes it tempting to explore the applicability of eqn. (A3) also to metallic systems.

Taking 'a' as the position of the first maximum in $g(r)$, $a \approx 0.18\ \sigma$ at which value $c(a) \approx \approx 1.215$. Inserting a local coordination number of 12 for a typical Lennard-Jones solid yields a value

of about 14.4 for the left-hand side (LHS) of eqn. (A.3). But also from the Reatto data, $c(r = 0) \approx -35$ and $S(0) \approx 0.041$ so that $\tilde{c}(q=0) = \dfrac{S(0)-1}{S(0)} \approx -23$, leading to a value of the right-hand side (RHS) of about 11 thus confirming that the Lennard-Jones $c(r)$ under the above conditions satisfies the Bhatia-March constraint (A.3) approximately.

Following the use of this *model* with pair potentials given by eqn. (A.1) consider next the RHS of eqn. (A.3) for liquid Ar near the triple point. Bernasconi and March [35] give then, from diffraction measurements $c(r = 0) = -33$ and $\tilde{c}(q=0) = -17$, which then gives for the RHS of eqn. (A.3) the value 15. With z taken to be 12, this gives $c(a)\big|_{T_m}$ from eqn. (A.3) as 1.25 which is gratifyingly close to the model value discussed above for the Lennard-Jones fluid.

Now turning to metallic systems we examine the results by Reatto et al. [25] obtained using a model potential to simulate liquid Al. Inserting the values they obtained for the relevant quantities into eqn. (A.3) gives for the RHS $(-49 - (-38) - 1) \approx -12$ while the left-hand side, taking $z = 10$ gives approximately -1.8.

Table A.1

Values of the Ornstein-Zernike function at the origin, both in *r*- and in *q*-space. All values are obtained from currently available X-ray or neutron diffraction experiments

Liquid metal	$-c(r = 0)$	$-\tilde{c}(k = 0)$
Na	43	41
K	42	40
Rb	45	42
Cs	50	38
Cu	60	47
Ag	51	53
Au	35	38
Mg	31	39
Al	45	54
Ga	34	200
Pb	44	110
Sn	40	140
Fe	46	48
Ni	41	50
Co	35	50

To conclude this Appendix, we note from Table (A.1) [36] that three liquid metals near freezing, namely Ga, Pb and Sn, show major deviations from the Percus-Yevick hard sphere prediction that the RHS of eqn. (A.3) is zero (see A.2). Evaluating the RHS. of eqn. (A.3) for these three metals using again diffraction data for $\tilde{c}(q=0)$ and $c(r=0)$ gives ~–170, ~–100 and ~–70 respectively. This predicts large negative values of $c(r)$ at the near-neighbour distance in the hot solid. It is an interesting matter for the future to construct $c(r)$ when suitable diffraction data becomes available for any one of these three metals near their freezing points. What then is the most inter-

esting consequence of the approximate prediction from eqn. (A.3) is the change of sign of $c(a)|_{T_m}$ in going from liquid Ar to the metals Ga, Sn and Pb. Whether eqn. (A.3) is sufficiently accurate quantitatively to yield coordination numbers seems less important than its qualitative consequence for the form of the direct correlation function $c(r)$. This, near T_m must at large r tend to $-\dfrac{\phi(r)}{k_B T}$ and it is of considerable interest to know at what value of r this asymptotic formula becomes a useful quantitative approximation for $c(r)$. Comparing Figs. (A1) and (A2) it is in evidence that this relation

$$c(r) \approx -\frac{\phi(r)}{k_B T} \tag{A.4}$$

at sufficiently large r is less evident for Al than for Ar.

APPENDIX B

Uncharged hard spheres direct correlation function

In order to obtain the pair correlation function $g(r)$ by direct Fourier transform of the experimental structure factor $S_{\exp}(q)$ one needs values of this structure factor for sufficiently high q-values. These high q-values are however not always available from experiment and one is forced to extend the diffraction data (see e.g. Reatto et al. [25]). It is therefore of considerable interest to examine possible analytic expression for the large q-behaviour of the static structure factor. In the Percus-Yevick approximation for hard spheres (HS) the direct correlation function $c_{HS}^{PY}(r)$ in r-space can be obtained analytically [37]. Below we examine its Fourier transform $\tilde{c}_{HS}^{PY}(q)$ in order to extract the leading term at large q. The leading term in the structure facor is then simply obtained using

$$S(q) = \frac{1}{1 - \tilde{c}(q)} \tag{B.1}$$

and we expect the expression resulting from this procedure to be appropriate to hard sphere like liquids such as Al.

We start from [37]

$$\begin{aligned} c_{HS}^{PY}(r) &= \alpha + \beta\left(\frac{r}{\sigma}\right) + \gamma\left(\frac{r}{\sigma}\right)^3 \quad r < \sigma, \\ c_{HS}^{PY}(r) &= 0 \quad r > \sigma \end{aligned} \tag{B.2}$$

with σ the HS diameter. In terms of the packing fraction $\eta = \dfrac{\pi}{6}\rho\sigma^3$, the coefficients in eqn. (B.2) are given by

$$\alpha = \frac{-(1+2\eta)^2}{(1-\eta)^4}, \qquad \beta = 6\eta\frac{\left(1+\frac{1}{2}\eta\right)^2}{(1-\eta)^4}, \qquad \gamma = -\frac{1}{2}\eta\alpha \tag{B.3}$$

Defining

$$\tilde{c}_{HS}^{PY}(q) = 4\pi\rho \int_0^\infty c_{HS}^{PY}(r) \frac{\sin(qr)}{qr} r^2 \, dr \tag{B.4}$$

we obtain

$$\frac{\tilde{c}_{HS}^{PY}(q)}{4\pi\rho} = -(\alpha+\beta+\gamma)\frac{\sigma\cos(\sigma q)}{q^2} + (\alpha+2\beta+4\gamma)\frac{\sin(\sigma q)}{q^3} +$$

$$+(2\beta+12\gamma)\frac{\cos(\sigma q)}{q^4\sigma} - \frac{2\beta}{q^4\sigma} - 24\gamma\left(\frac{\sin(\sigma q)}{q^5\sigma^2} + \frac{\cos(\sigma q)}{q^6\sigma^3} - \frac{1}{q^6\sigma^3}\right). \tag{B.5}$$

Terms in q^{-4} and q^{-6} come from non-analytic terms in r and r^3 at the origin $r = 0$ in $c(r)$ in eqn. (B.2). All other terms arise from the singularities of $c(r)$ at $r = \sigma$, as is evident from the fact that they have multiplicative factors $\sin(\sigma q)$ and $\cos(\sigma q)$. Fig. (B.1) shows $\tilde{c}_{HS}^{PY}(q)$ together with its leading term

$$-(\alpha+\beta+\gamma)\frac{\sigma\cos(\sigma q)}{q^2}. \tag{B.6}$$

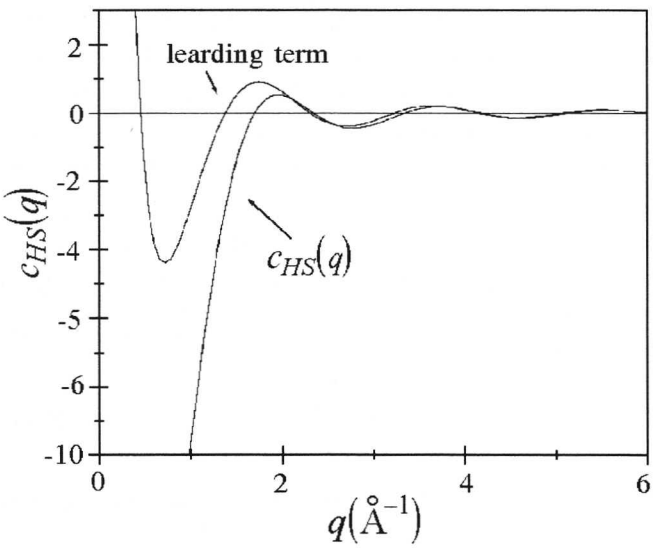

Fig. B.1. Direct correlation function of uncharged hard spheres in the Percus-Yevick approximation together with its leading term at large r

Using the above relations (B.2) and (B.3) Bhatia and March [38] prove that

$$\tilde{c}_{HS}^{PY}(q=0) - c_{HS}^{PY}(r=0) - 1 = 0 \tag{B.7}$$

and hence it follows that hard spheres in the Percus-Yevick approximation obey relation (A.3) trivially since $a \geq \sigma$ and thus $c_{HS}^{PY}(r) = 0$. We note however from Table (A.1) that the alkali metals, which are in section 0 supposed to be best described by an OCP-reference system, satisfy eqn. (B.7) very well.

1. *R. Winter, F. Hensel, T. Bodensteiner, W. Gläser, Ber Bun-Sénges*, J. Phys. Chem. **91,** 1327 (1987); J. Phys. Chem. **92**, 7171 (1988).
2. *R. Winter, F. Hensel*, Phys. Chem. Liquids **20**, 1 (1989).
3. *See also G.R. Freeman and N.H. March*, J. Phys. Chem. **98**, 9486 (1994).
4. *N.H. March*, Phys. Chem. Liq. **20,** 241 (1989), J. Math. Chem. **4**, 271 (1990).
5. *B.J.C. Cabral, J.L. Martins*, Phys. Rev. **B51,** 875 (1995).
6. *S.G. Brush, H.L. Sahlin, E. Teller*, J. Chem. Phys. **45**, 2102.
7. *For fully* quantitative work, see *J.P. Hansen*, Phys. Rev. **A8**, 3096 (1973); *S. Galam, J.P. Hansen*, Phys. Rev. **A14**, 816 (1976); see also *M.J. Gillan*, J. Phys. **C1** L1 (1974).
8. *F. Shimojo, Y. Zempo, K. Hoshino, M. Watabe*, Phys. Rev. **B55**, 5708 (1997).
9. *J.L. Martins*, Proceedings of the International Conference on Density Functional Theory and its applications to Materials held at the University of Antwerp (RUCA), June (2000).
10. *K.K. Mon, R. Gann, D. Stroud*, Phys. Rev. **A24,** 2145 (1981).
11. *G. Senatore, M.P. Tosi*, Phys. Chem. Liq. **11**, 365 (1982).
12. *V.A. Ivanov, I.N. Makarenko, A.M. Nikolaenko, S.M. Stishov*, Phys. Lett. **A47**, 75 (1974).
13. *W.G. Hoover, M. Ross*, Contemp. Phys. **12**, 339 (1971).
14. *D.A. Young*, 'Phase diagrams of the elements' University of California Press (1976).
15. *K. Tsuji*, Proceedings of the International Conference on High Pressure Science and Technonogy (Airapt 17) 25-30 July 1999 Honolulu Hawai'i and J. Non-Cryst. Solids **117** and **118** (1990) 27; and references therein.
16. *A. Ferraz, N.H. March*, Phys. Chem. Liq. **8,** 289 (1979).
17. *J.N. Glosli, F.H. Ree*, Phys. Rev. Lett. **82**, 4659 (1999) and references therein.
18. *F.P. Bundy*, J. Chem. Phys. **38**, 618 (1963); **38**, 631 (1963).
19. *S. Krishnan, D.L. Price*, J. Phys.: Condens. Matter **12**, R145 (2000).
20. *N. Vast, S. Bernard, G. Zerah*, Phys. Rev. **B52**, 4123 (1995).
21. *W. Jank, J. Hafner*, Phys. Rev. **B41** 1497 (1990).
22. *Y. Kita, J.B. Van Zytfeld, Z. Morita and T. Iida*, J. Phys.: Condens. Matter **6**, 811 (1994).
23. *C.A. Angell, S.S. Borick, M.H. Grabow*, J. Non-Cryst. Solids **205–207**, 463 (1996).
24. *E.P. Donovan, F. Spaepan F.D. Turnbull, J.M. Poate, D.C. Jacobson*, J. Appl. Phys. **57**, 1795 (1985).
25. *L. Reatto, D. Levesque, J.J. Weiss*, Phys. Rev. **A33**, 3451 (1986); See also *L. Reatto*, Phil. Mag. **A58,** 37 (1988).
26. *F. Perrot, N.H. March*, Phys. Rev. **A42**, 4884 (1990).
27. *R.C. Brown, N.H. March*, J. Phys. **C6**, L363 (1973).
28. *C.C. Matthai, P.J. Grout, N.H. March*, J. Phys. **F10**, 1621 (1980).
29. *K.S.C. Freeman, I.R. McDonald*, Mol. Phys. **26**, 529 (1973).
30. *R.H. Fowler*, Proc. Roy. Soc. London, Ser. A **159**, 229 (1937).
31. *N.H. March, M.P. Tosi*, Atomic Dynamics in Liquids Dover (1991).
32. *J.A. Alonso, N.H. March*, Surface Science **160**, 509 (1985).
33. *S. Munejiri, F. Shimojo, Kozo Hoshino*, J. Phys.: Condens. Matter **12**, 4313 (2000).
34. *L. Verlet*, Phys. Rev. **165**, 201 (1968).
35. *J.M. Bernasconi, N.H. March*, Phys. Chem. Liquids **15**, 169 (1986).
36. *N.H. March*, Phil. Mag. **A80**, 1335 (2000).
37. *E. Thiele*, J. Chem. Phys. **39**, 474 (1963); *M.S. Wertheim*, Phys. Rev. Lett. **10**, 321 (1963).
38. *A.B. Bhatia, N.H. March*, J. Chem. Phys. **80**, 2076 (1984).